

tions are fully exchanged with bivalent cations such as alkaline earth metal ions, six cations per unit cell are introduced.² When the cations are monovalent, twelve cations per unit cell are introduced.

The present crystal structures of dehydrated $\text{Sr}_{1.6}\text{Ti}_{8.8}\text{-A}$ and $\text{Sr}_{5.45}\text{Ti}_{11.1}\text{-A}$ indicate that Sr^{2+} ions preferentially occupy 6-ring sites and Ti^+ ions occupy 8-ring sites when the total number of ions per unit cell is more than 8. This result is reasonable considering ionic radii of $\text{Ti}^+(1.47 \text{ \AA})$ and that of Sr^{2+} ion (1.12 \AA).¹⁴ Larger Ti^+ ion will better fit to larger 8-ring site over 6-ring. These result are also consistent with those from the structures of $\text{Ag}_9\text{Cs}_3\text{-A}$,¹⁵ $\text{Ag}_9\text{Rb}_3\text{-A}$,¹⁶ $\text{Ag}_{6.5}\text{Ti}_{5.5}\text{-A}$,¹³ and $\text{Ag}_{9.3}\text{K}_{2.7}\text{-A}$.¹⁷ In those structures, larger Cs^+ , Rb^+ , Ti^+ , and K^+ ions are also associated with the 8-ring oxygens.

Acknowledgement. This work was supported by the Basic Research Institute Program, Ministry of Educations, Korea, 1989.

References

1. D. W. Breck, *Zeolite Molecular Sieves*, Wiley, New York, 1974.
2. K. Seff, *Acc. Chem. Res.*, **9**, 121 (1976).
3. The nomenclature refers to the contents of unit cell. For example, $\text{Na}_{12}\text{-A}$ represents $\text{Na}_{12}\text{Si}_{12}\text{Al}_{12}\text{O}_{48}$, exclusive of water molecules if a hydrated crystal is considered.
4. J. F. Charnell, *J. Cryst. Growth*, **8**, 291 (1971).
5. K. Seff and M. D. Mellum, *J. Phys. Chem.*, **88**, 3560 (1984).
6. Principal computer programs used in this study was Structure Determination Package Programs written by B. A. Frenz and Y. Okaya. These programs were supplied by Enraf-Nonius, Netherland, 1988.
7. R. L. Firor and K. Seff, *J. Am. Chem. Soc.*, **100**, 3091 (1978).
8. J. J. Pluth and J. V. Smith, *J. Am. Chem. Soc.*, **104**, 6977 (1982).
9. R. L. Firor and K. Seff, *J. Am. Chem. Soc.*, **99**, 4039 (1977).
10. D. S. Kim, S. H. Song and Y. Kim, *Bull. Korean Chem. Soc.*, **9**, 303 (1988).
11. *International Tables for X-ray Crystallography*, Vol. IV, Kynoch Press, Birmingham, England, pp. 73-87, 1974.
12. Reference 11, p. 149.
13. Y. Kim and K. Seff, *J. Phys. Chem.*, **82**, 1307 (1978).
14. *Handbook of Chemistry and Physics*, 67th Ed., Chemical Rubber Co., Cleveland, Ohio, 1986/1987, P F-198.
15. Y. Kim and K. Seff, *J. Phys. Chem.*, **92**, 5593 (1988).
16. Y. Kim, S. H. Song, D. S. Kim, Y. W. Han and D. K. Park, *J. Korean Chem. Soc.*, **33**, 18 (1989).
17. Y. Kim, S. H. Song, J. Y. Park and U. S. Kim, *Bull. Korean Chem. Soc.*, **82**, 1307 (1978).

Potential Profiles and Capacitances of an Ideally Polarizable Electrode in a point Charged Electrolyte

Sang Youl Kim* and K. Vedam†

Department of Physics, Ajou University, Suwon 441-749

†Materials Research Laboratory, The Pennsylvania State University, University Park, Pennsylvania 16802. Received October 11, 1989

The effects of the charged metal on the overall electrostatic potential profiles and the capacitances of the electrical double layer are brought out. A model with a simplified jellium and a point-charged electrolyte is utilized in the present calculations. Electrons are assumed not to penetrate electrode surface due to a strong screening of electrolyte at the interface. Electron density functions and ion density functions are obtained, which are also based upon the Poisson equation and Boltzmann equation on either side of the interface. A complete potential profile starting from bulk electrode and ending at bulk electrolyte is obtained by connecting the two potential profiles (one inside the metal electrode, the other inside the electrolyte) with proper boundary conditions. In spite of the simplicity of the model, the present model reveals the importance of the effect of the charged metal on the electrostatic potential profile and the electrical double layer capacitances. The results are discussed and compared with the predictions by Gouy Chapman theory.

Introduction

Since the early works of Gouy, Chapman and Stern (GCS),¹ considerable attention has been paid to the study of the electrical double layer by a number of researchers. Models for the study of one sided electrode interface mostly consist of an ideally polarizable electrode (IPE) which is perfectly flat and smooth, and an electrolyte. The electrolyte is treated as charged hard spheres immersed in a dielectric

continuum. Most of the studies have been devoted to improve the GCS theory of the electrical double layer, that is, on the electrolyte side by mean spherical approximation and its generalization,² the hypernetted chain approximation and its derivatives,³ the modified Poisson-Boltzmann and the Born-Green-Yvon type theories.⁴ On the other side of the electrical double layer, the effect of the charged electrode has been relatively neglected for the following suggested reasons. i) when a potential is applied to the electrode, the

metal surface forms a constant potential surface and the DC electric field inside the metal electrode is zero. ii) Hence, the potential difference, if it should exist, is made at the very surface of the metal with the surface charge density which can be determined by the electric field just outside the electrode surface, and iii) the thickness of this surface charge region, which is the same magnitude of Thomas-Fermi screening length, is extremely small ($\sim 0.5\text{\AA}$) compared to the corresponding thicknesses such as Debye-Hueckel lengths of electrolytes or semiconductors. Exceptions are one by Rice and that by Kofman *et al.*⁵ The latter showed the effect of the charged metal on the reflectance spectra by a simplified jellium model where electrons are bounded inside the metal electrode, and hence do not penetrate the metal/electrolyte interface. Quite recently, the electron density function of metal/vacuum interface is introduced into the electrode/electrolyte interface. But since proper corrections of strong screening of electrolyte is not introduced into the metal/vacuum theory, the effect of the charged electrode tends to be overemphasized.⁶ This density function of metal/vacuum interface inherently allows penetration of electron from metal into outside of metal, that is, into the electrolyte. The penetration of electron will not be the same at the metal/electrolyte interface as that at the metal/vacuum interface since the magnitude of the electron density of electrolyte is comparable to that of metal. In fact, there might be no penetration of electron at all if the electron density function of electrolyte is the same in magnitude and commensurate to that of the metal electrode.

In the present communication, therefore, no electrons are assumed to cross the boundary of metal/electrolyte either from metal to electrolyte or from electrolyte to metal. This model might be a better representation of the real electric double layer for the metal side, if one recognizes the strong screening of the electrolyte as is pointed out by Chao *et al.*⁷ Also it is clearly demonstrated that the effect of the charged metal electrode should not be neglected as its contribution to the potential profile and hence to the capacitance of the electrical double layer is proven to be critical.

Theory

For the evaluation of the electrical potential profile in the diffuse layer, the Gouy-Chapman (GC) model suggested by Gouy and Chapman¹ is adopted. The charge distribution function is determined in terms of the potential energy difference of the corresponding charged particles according to the Boltzmann distribution function. With some reasonable assumptions, such as the chemical potential of the bulk liquid is the same as that of the diffuse layer at the equilibrium state and that the DC dielectric constant of water is constant throughout the diffuse layer, the theory yields the exact analytic solutions to the potential and the charge distribution in the diffuse layer, for Z-Z electrolyte. Since the detailed derivation and the discussion can be seen elsewhere,⁸ only the results will be quoted here. The reference frame of coordinates is such that the distance is measured from the electrode/electrolyte boundary which forms an infinite plane at $x=0$. Then the potential profile can be represented by $\phi(x)$, with the boundary condition that ϕ is zero at infinity; thus $\phi(x)$ represents the potential difference between the bulk li-

quid and a point at a distance x from the boundary. The concentration function of species i and the potential function for Z-Z electrolyte are given explicitly by

$$C_i(x) = C \exp\left[(-Z_i e/kT)\phi(x)\right] \quad (1)$$

$$\phi(x) = \frac{4kT}{Ze} \tan^{-1} \left\{ \tanh \frac{Ze\phi(x_s)}{4kT} \exp\{-x(x-x_s)\} \right\} \quad (2)$$

where C is the bulk concentration of the electrolyte, Ze is the charge of the species, k is the Boltzmann constant, T is the temperature, $K = Ze(2C/\epsilon kT)^{1/2}$ is the reciprocal Debye-Hueckel length, ϵ is the permeability of the electrolyte, x_s is the thickness of constant concentration,⁹ and $Z = |Z_+|$. When the finite sizes of the ions are not negligible around $x=0$, a non-diffuse-like region is allowed in between the metal surface and the diffuse layer. One of the non-diffuse-like regions is the so called "Outer Helmholtz Plane (OHP)", which is generated from the model suggested by Stern.¹ In this paper the sizes of ions are not taken into account, thus explicitly visualizing the effect of the charged metal compared to GC theory. In other words, x_s is taken to be zero here. The effect of the finite size of ions is discussed in full detail elsewhere,¹⁰ hence will not be discussed any further here.

For the potential profile inside a metal, it is obvious that there cannot exist any DC electric field inside the conductor. When a potential is applied to a conductor the potential drop occurs at the surface of the conductor and the discontinuity of the electric field is directly related to the surface charge density through boundary conditions. The thickness of this charged surface layer, or in other words, the space charge region is negligibly small (Thomas-Fermi screening length). But in an electrolyte and semiconductors the thickness of the corresponding space charge region can range from a fraction of an angstrom to several thousand angstroms. In metals the thickness is a few tenths of an angstrom. Even though this region is very small, this region should not be neglected in the S/L interface study, because it plays a very important role in determining the potential profile throughout the metal electrode and the electrolyte.

The potential distribution as a function of x inside the metal can be obtained in a similar way as has been done by GC theory for the case of an electrolyte. However one thing that should be kept in mind is that there is only one kind of mobile charged particles in the metal, namely the electrons. Further the electron is known to have a negligible size ($< 10^{-13}$ cm).¹¹

Let $N(x)$ be the number of electrons per unit volume near the interface and N_0 be the bulk electron density of the metal, then the Poisson equation demands

$$-\frac{d^2}{dx^2} \phi(x) = -\frac{e}{K_m \epsilon_0} [N(x) - N_0] \quad (3)$$

where K_m is the dielectric constant of the metal and ϵ_0 is the vacuum permeability. Also using the Boltzmann distribution, the density of electrons can be written in terms of the potential $\Psi(x)$, the potential difference between $\phi(x)$ and ϕ_m , as

$$\begin{aligned} N(x) &= N_0 \exp\left[(e\phi(x) - e\phi_m)/kT\right] \\ &= N_0 \exp[e\Psi(x)/kT] \end{aligned} \quad (4)$$

where ϕ_m is the potential of the metal electrode with respect

to the bulk electrolyte, which can also be expressed as $\phi(-\infty)$. Following the standard procedure of solving the Poisson equations, it can be shown that

$$\frac{d\psi(x)}{dx} = -\text{sgn}(\phi_m) (2N_0 kT / K_m \epsilon_0)^{1/2} (\exp(e\psi(x)/kT) - 1 - e\psi(x)/kT)^{1/2} \quad (5)$$

where $\text{sgn}(\phi_m)$ denotes the sign of ϕ_m . This equation can be integrated by a numerical method to yield the x dependency of the potential inside the metal. Once the potential profile is obtained, the electron density profile can readily be obtained by using the potential profile with the Eq. (4). Also the surface charge density on the metal surface is obtained with the following equations.

$$\begin{aligned} \sigma &= -e \int_{-\infty}^0 (N(x) - N_0) dx \\ &= \text{sgn}(\phi_m) (2K_m \epsilon_0 kT N_0)^{1/2} (\exp(e\psi(0)/kT) - 1 - e\psi(0)/kT)^{1/2} \quad (6) \end{aligned}$$

The surface charge density of the metal surface, which is calculated by integrating the excess volume density of electrons, is found to have an one-to-one correspondence with $\psi(0)$ in Eq. (6) or equivalently, the surface potential $\phi(0)$. Thus a nonzero potential profile inside the metal exists as far as the surface charge density does not vanish. Therefore, since the surface charge density is always nonzero except at the potential of zero charge (PZC), it is seen that the potential profile inside the metal always exists and is essential in determining the overall potential profile and capacitance of the electric double layer.

In order to complete the calculation of the potential profile, the potential at the metal electrode/electrolyte interface ($x=0$) is determined by the following two boundary conditions:

$$\phi(x=0_-) = \phi(x=0_+) \quad (7)$$

$$K_m \epsilon_0 d\psi/dx(x=0_-) = \epsilon d\phi/dx(x=0_+) \quad (8)$$

Eq. (7) is the continuity condition of the potential and Eq. (8) means the continuity of the magnitude of the electric displacement D at $x=0$. The latter condition can be derived by applying Gauss' theorem with the help of Eqs. (3) and (6); explicitly, we equate the surface charge of the metal calculated from the metal side as shown in Eq. (6), to the net surface charge density of the ions in the electrolyte calculated from liquid side as follows

$$\begin{aligned} \sigma &= -\epsilon d\phi/dx(x=0_+) \\ &= \text{sgn}(\phi_m) (8kTC\epsilon)^{1/2} \sinh\{Ze\phi(0)/2kT\}. \quad (9) \end{aligned}$$

With the Eqs. (6) to (9) for the Z-Z electrolyte, it can be shown that the potential at the boundary or $\phi(0)$ should satisfy the following condition.

$$\begin{aligned} \exp\{(e\phi(0) - e\phi_m)/kT\} - 1 - e(\phi(0) - \phi_m)/kT \\ = (4\epsilon C/K_m \epsilon_0 N_0) \sinh^2\{Ze\phi(0)/2kT\} \quad (10) \end{aligned}$$

A numerical method is employed to get the value of $\phi(0)$ from Eq. (10). Once $\phi(0)$ is evaluated, the potential profile and

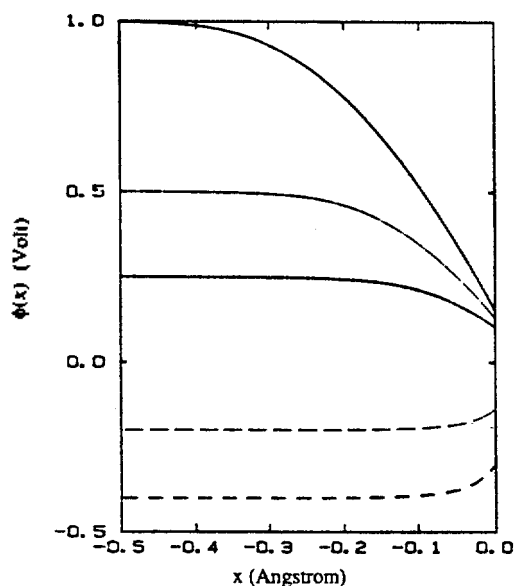


Figure 1. Calculated potential profiles of gold in 0.1M potassium chloride solution as a function of distance x inside the gold electrode for potential differences of 1.0 V (solid line), 0.5V (— — —), 0.25V (— · — · —), -0.2V(— · —) and -0.4V (· · ·).

charge concentrations in the metal electrode as well as in the electrolyte are obtained from the corresponding equations. The capacitance of the electrical double layer is then calculated from the ratio of the charge on the metal electrode to the potential difference.

Results and Discussion

For the electron density N_0 of the electrode, that of single crystal gold ($5.9 \times 10^{22}/\text{cm}^3$) is used.¹¹ The concentration C of the potassium chloride solution is 0.1 M, which simulates the electrolyte. The dielectric constant of electrolyte is assumed to be constant throughout the electrolyte region and K_m is approximated to 1. The specific adsorption, which can be defined either as a depletion of the solvation sheath at least partially in the direction of the electrode¹² or the adsorption of anions at the negatively charged electrode,⁸ is not taken into account.

The potential profiles inside the electrode for a few potential differences between the electrode and the bulk liquid as a function of distance x are presented in Figure 1. The variation of the potential inside the electrode is seen within a few tenths of an angstrom. These variations in the potential even though they occur in an extremely thin surface layer, are not negligible and hence should be incorporated in the investigations of double layer properties for the reasons given below. The portion of the potential change inside the electrode becomes significant as the potential increases along an anodic (positive) direction as can be seen from Figure 1 and 2. When the potential difference between the electrode and bulk electrolyte is 1.0 volt, about 70~85% of the potential drops inside the electrode, thus leaving the potential drop from the electrode/electrolyte interface to the bulk liquid about 0.15~0.30 volt depending the bulk concentration of electrolyte. That is, the voltage drop in the liquid is only 15~30%. The relative amount of the potential drop which occurs inside the electrode is not constant but depends on

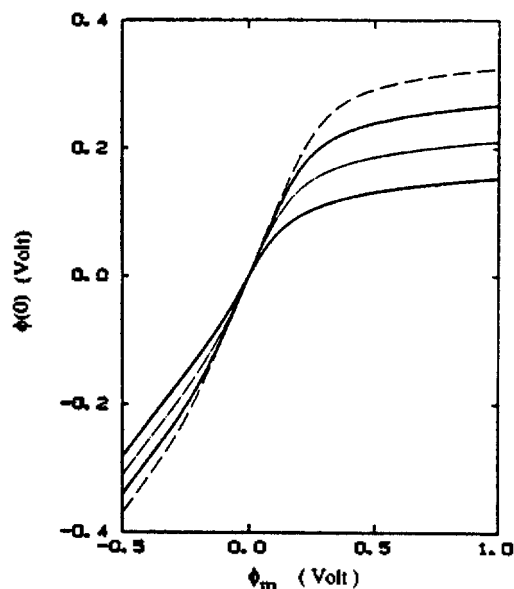


Figure 2. The potential at the gold/liquid interface ($x=0$) as a function of potential difference between gold electrode and liquid for 0.1M (solid line), 0.01M (---), 0.001M (-·-·-), and 0.0001M (·-·-·) of potassium chloride solution.

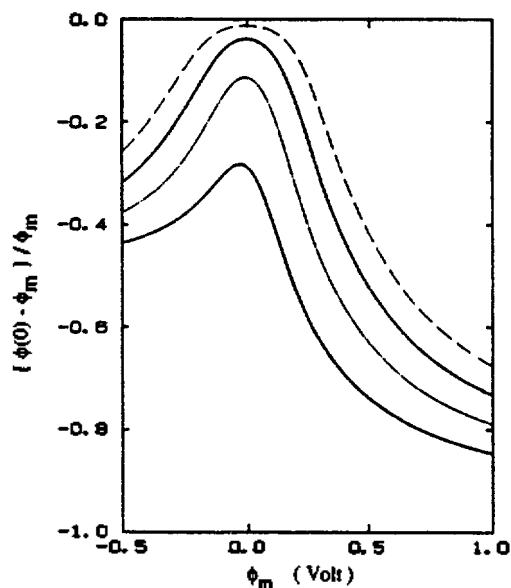


Figure 3. The relative potential drop $(\phi(0) - \phi_m) / \phi_m$ at the gold/liquid interface ($x=0$) as a function of potential difference between gold electrode and electrolyte for 0.1M (solid line), 0.01M (---), 0.001M (-·-·-), and 0.0001M (·-·-·) of potassium chloride solution.

the magnitude and the polarity of the potential difference between the electrode and the bulk liquid. The absolute potential in volts and the relative potential at the electrode/electrolyte interface are presented in Figure 2 and 3 respectively. The amount of variation in the potential inside the metal electrode increases as potential deviates from PZC. Also around the PZC and at lower concentration of electrolyte, the potential change inside the metal electrode is small (~5% for 0.001 M around PZC), thus the entire potential occurs at the electrical diffuse layer as predicted by GC theory. In Figure 4 the electron density profiles are shown as a function of distance x for a few selected potential dif-

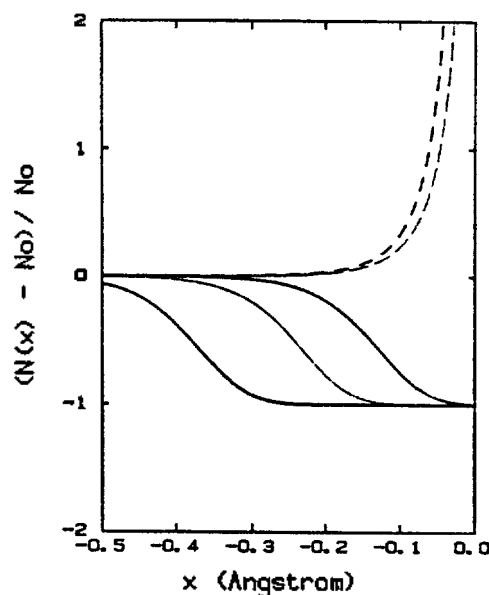


Figure 4. The relative electron density as a function of distance for a few selected potential difference of 1.0V (solid line), 0.5V (---), 0.25V (-·-·-), -0.2V (---) and -0.4V (·-·-·) between gold electrode and electrolyte. Positive means accumulation of electrons and negative means a depletion of electrons.

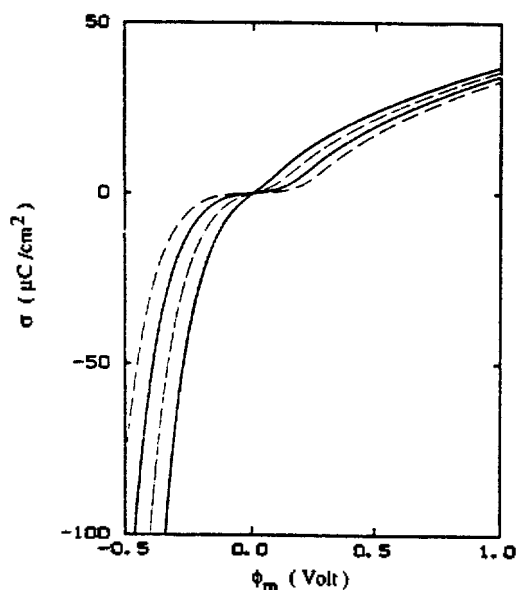


Figure 5. The calculated surface charge density on the gold electrode vs potential difference between gold electrode and electrolyte for 0.1M (solid line), 0.01M (---), 0.001M (-·-·-), and 0.0001M (·-·-·).

ferences. For the positive potential, the thickness of the electron depletion layer is seen to increase as the potential increases, thus attributing most of the potential difference to that in the electron depleted region. On the other hand, for the negative potential the potential drop inside the electrode is not so dominating. The potential change inside the liquid is bigger than that inside the electrode. The thickness of the electron accumulation layer is nearly constant at $\sim 0.1\text{\AA}$, only the electron density at $x=0$ increases explosively as the magnitude of the potential increases. As is shown from

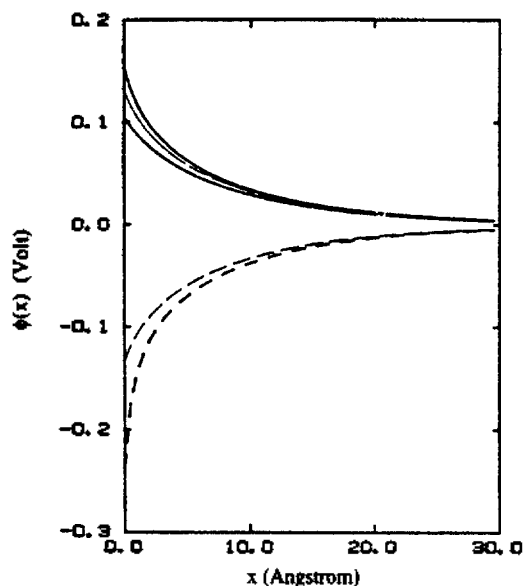


Figure 6. Potential profile inside the liquid for potential differences of 1.0V (solid line), 0.5V (---), 0.25V (-----), -0.2V (— · —) and -0.4V (···), between gold electrode and electrolyte.

the surface charge density of the electrode as a function of the potential in Figure 5, the surface charge density is a slowly increasing function of potential above ~ 0.2 volt and is a rather rapidly decreasing function below ~ 0.2 volt.

It is observed that there are asymmetries in the potential profile, the electron density profiles, and especially surface charge density around PZC. The asymmetries originate mostly from the physical properties of the charge carriers, the negatively charged electrons with a finite volume density, which is the only kind of charge carrier in the electrode. For a negative potential, the electrons will accumulated without limit in a very narrow region, as far as it is energetically allowed. This will favor an increase of the surface charge density, but the potential do not increase so abruptly because it should increase in an ultra narrow region. On the other hand, for the positive potential the electrons are depleted from the interface and the depth of the electron depletion layer can increase rather easily. Thus the amount of the potential drop increases quadratically with the thickness of the depleted region, resulting in a slower increase of the surface charge density but a bigger potential drop inside the electrode. Since the capacitance per unit area is the surface charge density divided by the applied potential, the behavior of the surface charge density and the potential drop inside the electrode as a function of applied potential are directly reflected in the behavior of the electrical double layer capacitance. A more detailed discussion of the double layer capacitance follows.

The large potential drop inside the electrode implies that the electric field in the inner Helmholtz layer is not necessarily large as had been estimated so far.^{8,9} Especially for the positive potential, the potential drop in the liquid has relatively small portion of the potential difference between the electrode and the liquid, even though the potential difference increases continuously, thus keeping the magnitude of the electric field in the inner Helmholtz layer low. The potential profile in the diffuse layer is plotted in Figure 6. As the potential profile and the charge distribution are known, it is a

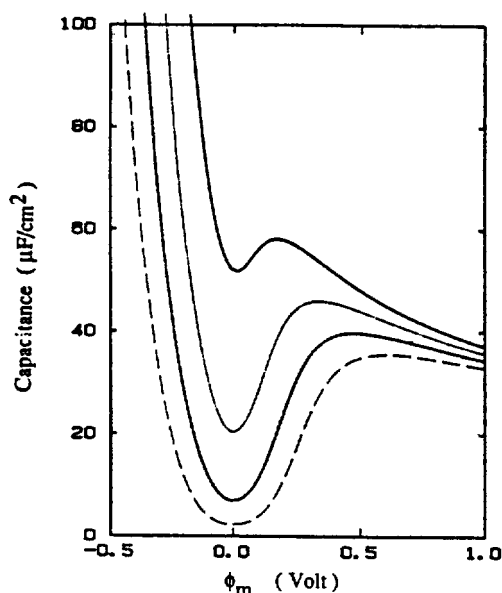


Figure 7. Capacitance of a double layer of gold in 0.1M (solid line), 0.01M (---), 0.001M (-----), and 0.0001M (···) potassium chloride solution vs potential difference between gold electrode and electrolyte.

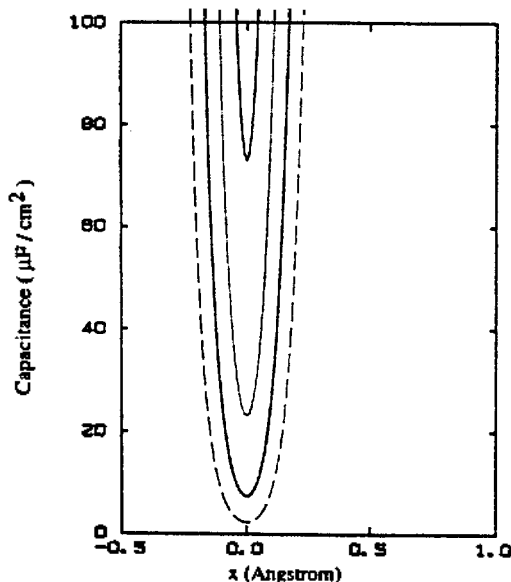


Figure 8. Capacitance of a double layer of gold in 0.1M (solid line), 0.01M (---), 0.001M (-----), and 0.0001M (···) potassium chloride solution vs potential difference between gold electrode and electrolyte, by GC theory.

straightforward procedure to calculate the capacitance of the double layer. The capacitance of the electrical double layer as a function of potential is presented in Figure 7.

A comparison of capacitances with those by GC theory reveals a few points worth mentioning. First, the capacitances in Figure 7 never diverge as they do according to the diffuse layer theory (Figure 8) when the potential deviates from the PZC.^{8,9} At the PZC, a minimum in either the capacitance curve or the differential capacitance curve versus potential is observed in both the theory. The reason for the disappearance of the exploding behavior of the capacitance off the PZC in the present model is mostly

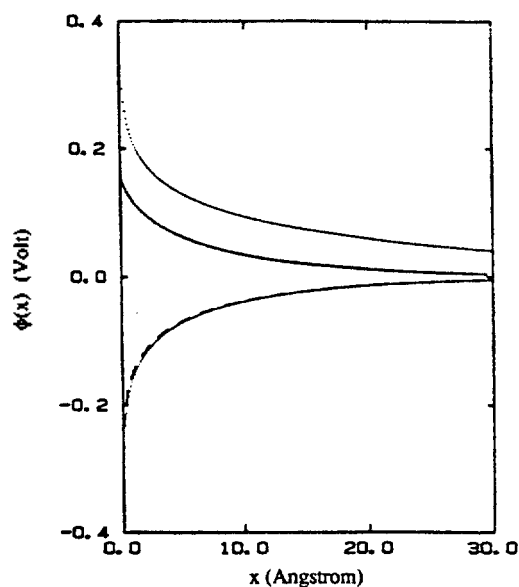


Figure 9. Potential profile inside the liquid for potential differences of 1.0V (solid line), and -0.4V (-), between gold electrode and electrolyte. (those by GC theory are plotted as dots for comparison).

due to the effect of the metal electrode. Explicitly, for a positive potential, the exponential increase of the charge observed in the diffuse layer theory is restricted by the increase in the thickness of the electron depletion layer, which is necessary to keep electrical charge neutrality at the interface. The potential is an approximately quadratic function of distance x inside this electron depletion layer. Hence, the surface charge density is kept low and the capacitance does not exhibit explosive behaviors. This is well observed in Figure 9. For a negative potential, the electrons are rather easily accumulated at the metal surface at low potential. This explains why the capacitance rises up very quickly at a negative potential as shown in Figure 7 and the two potential profiles in Figure 9 are quite similar to each other for a negative potential. However, as the magnitude of the potential increases, it is more difficult to accumulate additional electrons in the ultra narrow region of 0.1Å (Figure 4), against the electrostatic repulsion, thus the capacitance increases less explosive. Another results to be noticed is that when electrolyte bulk concentration is high, the minimum capacitance at PZC in Figure 7 is much smaller than that evaluated by the GC theory in Figure 8. As the experimental capacitances at PZC are even smaller than those predicted by the present theory, the present theory is believed to be on the right track. As the solution gets more diluted, the predictions by the present model are quite close to those evaluated by diffuse layer theory. For example, the slope of $\phi(0)$ vs ϕ_m is about 1 (Figure 2), and minimal deviation of $\phi(0)$ from ϕ_m is shown (Figure 3) and the capacitance curve is quite similar to that by diffuse layer theory (Figure 7 and 8).

According to the present model, a metal is described in terms of its electron concentration and its dielectric constant. Since these two constants do not vary significantly among metals, the potential profile inside the metal electrode will not differ so much from one kind of metal to another. Also it is believed that the total potential change inside the metal will not depend greatly on the model of the metal electrode under DC electric field. Thus the present model, which can be de-

scribed as a simplified jellium model with bixed nuclei forming a rigid structure and electrons being confined inside the electrode, that is, the model with no penetration of electrons from and/or into $x < 0$ region, is strongly believed to predict the correct response of the metal electrode under a DC field.

Further improvements of the present model can be achieved in two ways. First, since the ions in the electrolyte have finite sizes, these size effect should be included in the model. This can be done by inserting intermediate layers of constant concentration between the metal electrode and the electrical diffuse layer. One such constant concentration layer is the well known Stern layer, whose thickness could be the radius of hydrated counter ion. Another constant concentration layer is that of the saturated counter ion. This layer will exist since the concentration of hydrated counter ion at just outside of the OHP, cannot exceed a certain value, which might be determined from the closest packing density of hydrated counter ion or the density of single crystal, composed of the same element. The thickness of this saturated layer will be a function of the potential difference, the size of hydrated counter ion, and the bulk concentration of the electrolyte. This layer will be located between Stern layer and the electrical diffuse layer. Once these constant concentration layers are added, there will be additional potential drop inside these layers, thus the total amount of potential drop inside the metal electrode and the electrical diffuse layer will be smaller. Accordingly, the surface charge density and capacitances will be smaller than those by present approach. The effect of these constant concentration layer will be dominating especially at the cathodic (negative) potential, where the rapid increase of the surface charge density as the electrode becomes more cathodic will be greatly suppressed. The size effects of ions will be discussed in a greater detail elsewhere.¹⁰

Second, as is implicitly suggested by Martynov *et al.*,⁶ the electrode/electrolyte interface boundary can possibly be pushed to the electrolyte. This shift of the boundary wall, even if it might be extremely small, will greatly affect the potential profile especially at cathodic potential. Although the thickness of this electronic contribution is assigned to be that of Stern layer by Martynov *et al.*,⁶ the electronic contribution is implied to be due to those electrons which are displaced to the new boundary of metal electrode. This electron might not be the same electrons which make penetration from metal into vacuum in the metal/vacuum interface theory.

Acknowledgement. The authors gratefully acknowledge the support of this research work by the National Science Foundation through the Grant No. DMR-8812824. One of the authors (SYK) would also like to acknowledge the Research Fellowship Grant from the Johnson Wax Fund, in the early stages of this work.

References

1. G. Gouy, *J. Phys.* 9(4), 457 (1910); D. C. Chapman, *Philos. Mag.*, 25, 475(1913); O. Stern, *Z. Electrochem.*, 30, 508 (1924).
2. Eric Y. Sheu, Chuan-Fu Wu, Sow-Hsin Chen, and Lesser Blum, *Phys. Rev. A* 32, No.6, 3807 (1985).
3. M. Lozada-Cassou, R. Saavedra-Berrera and D. Henderson, *J. Chem. Phys.*, 77, 5150 (1982).

4. D. Bratko, L. B. Bhuiyan, and C. W. Outhwaite, *J. Phys. Chem.*, **90**, 6248 (1986); C. W. Outhwaite, and L. B. Bhuiyan, *J. Chem. Phys.*, **84**(6), 3461 (1986); Christopher, W. Outhwaite, *J. Chem. Soc., Faraday Trans.*, **2**, **82**, 789 (1986); C. Caccamo, G. Pizzimenti, and L. Blum, *Phys. Chem. Liq.*, **14**, 311 (1985); *J. Chem. Phys.*, **84**(6), 3327 (1986).
5. O. Rice, *Phys. Rev.*, **31**, 1051 (1928); R. Kofman, R. Garigos, and P. Cheyssac, *Thin Solid Films* **82**, 73 (1981).
6. Wolfgang Schmickler and Douglas Henderson, *J. Chem. Phys.*, **85**(3), 1650 (1986); G. A. Martynov and R. R. Salem, *Lecture Notes in Chemistry*, Vol. 33; "Electrical Double Layer at a Metal-dilute Electrolyte Solution Interface", Springer-Verlag, New York (1983); Ezequiel Leiva and Wolfgang Schmickler, *J. Electroanal. Chem.*, **229**, 39 (1987); A. Hamelin, L. Stoicoviciu, and F. Silva, *J. Electroanal. Chem.*, **229**, 107 (1987).
7. F. Chao, M. Costa, R. Cherrak, J. Lecouer, and J. P. Bellier, *J. Electroanal. Chem.*, **229**, 19 (1987).
8. J.O'M. Bockris, B. E. Conway, and E. Yeager, *Comprehensive Treatise of Electrochemistry*, Vol. 1: "Double Layer", Chap. 3, Plenum Press, New York and London (1980); A. W. Adamson, *Physical Chemistry of Surfaces*, 4th ed., Chap. 5, John Wiley & Sons, Inc., New York (1982).
9. D. M. Mohilner, *Electroanalytical Chemistry*, Vol.1, "The Electrical Double Layer, Part I." ed. A. J. Bard, Chap. 3, Marcel Dekker, Inc., New York (1966).
10. S. Y. Kim (Ph.D. Thesis, Pennsylvania State University).
11. C. Kittel, *Introduction to Solid State Physics*, 5th ed., John Wiley & Sons, Inc., New York (1976).
12. D. M. Kolb, *J. Vac. Sci. Technol.*, **A4**(3), 1294 (1986); D. M. Kolb, and J. Schneider, *Surf. Sci.*, **162**, 764 (1986).

¹³C NMR Study of the Application of the "Tool of Increasing Electron Demand" to the 9-Aryl-tricyclo[3.3.1.0^{2,5}]non-9-yl, and 8-Aryl-Tetracyclo[3.2.1.0^{2,7}.0^{4,6}]oct-8-yl cations

Wie-Chang Jin, Gweon-Young Ryu, Chun Yoon, and Jung Hyu Shin*

Department of Chemistry, Seoul National University, Seoul 151-742. Received October 12, 1989

The ¹³C NMR shifts of a series of para-substituted 9-aryl-tricyclo[3.3.1.0^{2,8}]non-9-yl and 8-aryl-tetracyclo[3.2.1.0^{2,7}.0^{4,6}]oct-8-yl cations were measured in FSO₃H/SO₂ClF at -90 °C or -70 °C in order to examine whether the ρ^{c+} values can be used to explain the mechanism for the stabilization of the geometrically rigid cyclopropylcarbinyl cations. Plots of the Δδ^{c+} shifts against σ^{c+} reveal excellent linear correlation. The tricyclononyl systems yield a ρ^{c+} value of -4.95 with a correlation coefficient *r* = 0.9948. The tetracyclo-octanyl systems give a ρ^{c+} value of -6.39 with *r* = 0.9943. A fair parallelism exists between the results of ¹⁹F nmr studies and the change of ρ^{c+} values in these cations. Accordingly, the present study established that the ρ^{c+} value can be used as a measure of the geometric influence for the charge delocalization in cyclopropylcarbinyl cations.

Introduction

The use of the Hammett σ and Brown σ⁺ substituent constants in the investigation of structure-reactivity relationships is well established¹. These substituent constants provide a measure of the stabilizing effect of the substituent on the reaction center of the transition state in the solvolytic and related reaction. On the basis of the usual assumption of a late transition state² in such solvolytic reactions, it was reasonable to anticipate that these constants could also be used to correlate that stabilities of the carbocationic intermediates produced in such solvolyses.

In recent years it has become possible to prepare and observe such carbocations in superacid media³. The ¹³C NMR chemical shifts in such carbocations have been taken to measure the electron delocalization of the carbocation. Accordingly, numerous attempts seeking to correlate the ¹³C NMR shifts with σ⁺, electrophilic substituent constant, have been reported⁴.

On the assumption of (i) a late transition state for the

solvolytic of cumyl chlorides in acetone and (ii) that the ¹³C chemical shifts were linearly proportional to charge density, it was not unreasonable to expect the σ⁺ constants to correlate ¹³C shifts of the fully formed carbocations in superacid. Thus Olah and coworkers plotted the ¹³C cationic carbon chemical shifts δC⁺ of cumyl cations against the electrophilic substituent constant(σ⁺) and noted an approximate linear correlation⁵. In a reinvestigation of the behavior of the substituted *tert*-cumyl cations, Kelly and Spear⁶ observed a lower correlation coefficient, *r* = 0.967. Even more importantly, they pointed out that the least-square line for their data failed to pass through the point for the parent *tert*-cumyl cation. They suggested that the discrepancy might be due to an enhanced charge delocalization in ions containing electron donating substituents.

Therefore, Brown⁷ and coworkers proposed the following modified Hammett-Brown equation of the form

$$\Delta\delta^{c+} = \rho^{c+} \sigma^{c+}$$

where Δδ^{c+} is the difference between the cationic carbon